

First-principles study of phosphorus and nitrogen impurities in ZnSe

K. W. Kwak* and David Vanderbilt

Department of Physics and Astronomy, Rutgers University, Piscataway, New Jersey 08855-0849

R. D. King-Smith

Biosym Technologies, Inc., 9685 Scranton Road, San Diego, California 92121

(Received 27 January 1995; revised manuscript received 21 June 1995)

Phosphorus and nitrogen defects in ZnSe have been studied by pseudopotential total-energy calculations. Various charge states of the phosphorus and nitrogen impurities occupying zinc sites (antisite defects) and interstitial sites (interstitial defects) were considered; their structural and electronic properties were investigated, and formation energies were calculated as a function of Se and electronic chemical potentials. The calculated electronic properties and formation energies were used in the investigation of the role of impurities in the p -type doping problem of ZnSe. Our study suggests that the difficulty with p -type doping of ZnSe by phosphorus results from the compensation of the shallow acceptors by the antisite defects P_{Zn} which act as triple donors. In the case of nitrogen, the concentrations of the antisite and interstitial defects are too low to cause such compensation, which is consistent with the successful p -type doping of ZnSe with nitrogen.

I. INTRODUCTION

Current interest in the use of wide-band-gap II-VI semiconductors is centered on the fabrication of blue diode lasers.¹ The development of reliable and inexpensive blue diode lasers is technologically and commercially very important, since they will provide significant benefit to virtually any technology that uses coherent visible light. Among II-VI semiconductors, ZnSe has been considered for a long time to be a very promising candidate for this purpose. With a direct band gap of 2.67 eV at room temperature, ZnSe has very efficient luminescence in the blue spectral region.

However, the fabrication of the p - n junctions essential to light-emitting devices has been hindered in II-VI semiconductors by doping difficulties. Most wide-band-gap II-VI semiconductors (including ZnSe) can easily be doped n type but resist p -type doping, while ZnTe can easily be doped p type but not n type. After two decades of effort directed towards obtaining highly conductive p -type ZnSe material, high enough hole concentrations for the fabrication of diode lasers ($\sim 10^{18} \text{ cm}^{-3}$) have recently been achieved in ZnSe using nitrogen free radicals as the doping source.² Subsequently, several groups^{3,4} have succeeded in demonstrating ZnSe-based semiconductor diodes that lase in the blue-green region of the visible spectrum.

In spite of this success in fabricating low-resistivity p -type ZnSe, the origin of the doping difficulties remains unclear. A number of explanations for the problem have been suggested.⁵⁻¹⁵ The most commonly accepted explanation has been that native defects (e.g., Zn self-interstitials) that act as donors are activated as a result of the doping, resulting in compensation of the acceptor impurities. However, recently Laks *et al.*¹⁶ employed *ab initio* total-energy calculations to investigate

self-compensation by native defects in ZnSe, and suggested that native-defect concentrations in stoichiometric ZnSe were too low to cause compensation. They also find that substantial concentrations of native defects are expected for both n -type and p -type doping in nonstoichiometric material, and are thus not able to explain the n -type preference of ZnSe. Also, this mechanism would predict the impossibility of p -type doping regardless of dopant, which seems inconsistent with the success of p -type doping of ZnSe using nitrogen. Thus, the native-defect self-compensation mechanism alone probably cannot explain the doping problem. Therefore, a detailed study of the role of impurities is necessary in order to understand this problem.

We have studied phosphorus and nitrogen impurities in ZnSe, using first-principles pseudopotential total-energy calculations, to investigate the problems associated with p -type doping. Our previous calculations¹⁷ have shown that substitutional nitrogen and phosphorus impurities on the Se site form shallow acceptors. Here, we report on calculations for P and N impurities in antisite and interstitial defect configurations. (Some results on the phosphorus defects have already appeared previously.¹⁸) The formation energies and the electronic and structural properties of the defects in their various charge states have been calculated. The results are used to interpret the role of impurity defects in the p -type doping difficulty of ZnSe.

We find that the antisite defect P_{Zn} plays a critical role in the p -type doping problem. When the Fermi level is near the valence-band maximum (VBM), the formation energy of P_{Zn}^{3+} in phosphorus-doped stoichiometric ZnSe is comparable to or lower than that of substitutional phosphorus P_{Se} . This suggests that, in the process of doping ZnSe p type with phosphorus, the shallow acceptors are compensated by the antisite defects, which can act as triple donors. In contrast, in the case of

nitrogen-doped stoichiometric ZnSe, the antisite defect N_{Zn} is predicted to have a higher formation energy than N_{Se} for the whole range of Fermi level, consistent with the successful fabrication of *p*-type ZnSe material based on nitrogen doping.

This manuscript is organized as follows. In Sec. II, the theoretical methods employed in this study are described. In Sec. III, the calculational results are presented and discussed. We first summarize the stable ionic configurations of defects in their various charge states. Calculational results of the electronic properties and formation energies of phosphorus and nitrogen defects follow. The results are then discussed in the context of the doping problem of ZnSe. Finally, we summarize in Sec. IV.

II. THEORETICAL METHODS

A. Total-energy calculations

Our theoretical approach is reviewed in this section. We employed a plane-wave pseudopotential approach within the local-density approximation for studying the energetics and the electronic properties of point defects in ZnSe.

Total-energy calculations with norm-conserving pseudopotentials have been successfully applied to the study of various solid-state systems.¹⁹ In the case of ZnSe, however, the highly localized *3d* orbitals of Zn present a severe challenge for the use of traditional norm-conserving pseudopotential approaches using plane-wave basis sets. The condition of norm conservation places a severe restriction on the form of the pseudo wave function, and makes it impossible to construct a pseudo wave function that is much smoother than the all-electron one. Consequently, the norm-conserving pseudo wave functions of the Zn *3d* states require a large number of plane waves in the basis set. The Zn *3d* states may be included in the core shell, but this results in a poor description of bulk ZnSe. For example, previous work on ZnSe and ZnS has shown^{20–22} that the inclusion of Zn *3d* states in the core shell can lead to errors on the order of 10% in the equilibrium lattice constant.

In our calculations, the occupied Zn *3d* states are treated in the *valence shell* using the ultrasoft pseudopotential scheme developed by Vanderbilt.²³ This approach overcomes the problem of the tightly bound states by relaxing the norm-conservation constraint and introducing a generalized eigenvalue formalism. Using the present scheme, we obtain good structural properties of bulk ZnSe with a plane-wave cutoff of only 25 Ry, yet we can still calculate forces on the atoms so as to relax atomic coordinates efficiently for the defect structures.^{17,24} For the case of nitrogen impurities, the problematic N *p* states can be treated as easily as those of the heavier column-V dopants within this scheme. For the exchange-correlation potential, we used the Ceperley-Alder form as parametrized by Perdew and Zunger.²⁵

32-atom and 33-atom bcc supercells were used in the defect calculations. A 32-atom supercell containing the formula unit $Zn_{15}Se_{16}X$ ($X = N$ or P) per 32-atom was

used for the antisite defect calculation to represent an isolated defect. For the interstitial defect calculation a 33-atom bcc supercell was used with the formula unit $Zn_{16}Se_{16}X$ per 33-atom cell. We fixed the lattice constant of the cell to be the experimental one.

The integration over the supercell Brillouin zone was approximated by a special \mathbf{k} point²⁶ $\frac{2\pi}{b}(\frac{1}{2} \frac{1}{2} \frac{1}{2})$ for systems with T_d symmetry, where b is the lattice constant of the supercell (11.34 Å). For a system with C_{3v} geometry, the equivalent set of \mathbf{k} points would consist of the two points $\frac{2\pi}{b}(\frac{1}{2} \frac{1}{2} \frac{1}{2})$ with weight $\frac{1}{4}$, and $\frac{2\pi}{b}(-\frac{1}{2} \frac{1}{2} \frac{1}{2})$ with weight $\frac{3}{4}$. However, for the bcc cell these two \mathbf{k} points are related by a reciprocal lattice vector $\frac{2\pi}{b}(1 0 0)$; thus only one \mathbf{k} point was needed even for a system with C_{3v} geometry. A similar argument holds also for a system with C_{2v} geometry. Tests with denser \mathbf{k} point sets indicate that the total energy is reasonably converged with the \mathbf{k} point set we used.¹⁷

To obtain the minimum-energy structure for each defect in ZnSe (for example, P_{Zn}^0), we started with an arbitrary configuration of the ions in a supercell that simulates the defect system. Using a conjugate-gradient minimization technique,^{27,28} the Kohn-Sham energy functional was minimized to obtain the electronic ground state for the fixed ionic configuration, and the Hellmann-Feynman forces on the ions were calculated. Then the ionic coordinates in the unit cell were updated using the forces as a guide. This procedure was repeated until the forces were negligible (less than 0.05 eV/Å).

B. Defect formation energies

Following the method suggested by Qian, Martin, and Chadi,²⁹ we have calculated the formation energies of defects in ZnSe as a function of the Fermi level and the Se chemical potential. We illustrate the formalism with P defects, but the argument and formulas below are valid for N defects also. The formation energy $F(D^Q)$ of a defect D^Q in charge state Q is a function of both electron chemical potential (or Fermi level) μ_e and atomic chemical potentials μ_{Zn} , μ_{Se} , and μ_P . However, since each defect system contains a P impurity, we can redefine the formation energy and omit μ_P . Furthermore, using the constraint that $\mu_{Zn} + \mu_{Se}$ is fixed by the total energy E_{ZnSe} of the two-atom unit of bulk ZnSe, we obtain

$$F(D^Q) = E(D^Q) + Q(\mu_e + E_v) - N_{Zn}E_{ZnSe} + (N_{Zn} - N_{Se})\mu_{Se}, \quad (1)$$

where $E(D^Q)$ is the total energy of the supercell for the defect system containing N_{Zn} zinc atoms and N_{Se} selenium atoms. The allowed range for μ_{Se} is given by

$$\mu_{Se}^{bulk} - \Delta H_f \leq \mu_{Se} \leq \mu_{Se}^{bulk}, \quad (2)$$

from the consideration of thermodynamic constraints. Our calculated value of the heat of formation of ZnSe is 2.79 eV. The Fermi level μ_e is measured relative to E_v , the top of the valence band in the bulk ZnSe crystal.

The energy in the defect cell corresponding to the top

of the valence band in bulk ZnSe has been determined by aligning the screened local potential at the atomic site farthest from the impurity atom with the potential at the site of the same kind in bulk ZnSe. If the cell was large enough, the local potential at the farthest atomic site would correspond to a bulk calculation, giving the exact value of E_v . When the cell used is not large enough, however, the local potential is different from that of the bulk calculation, and thus introduces an error in E_v . The estimated error in E_v in our 32-atom cell calculations is 0.1–0.2 eV.

When the formation energies of different types of defects are compared, we must consider the energies as a function of the Fermi level μ_e and the Se chemical potential μ_{Se} . However, for a specific type of defect, the relative formation energies for different charge states depend only on the Fermi level μ_e ; the (thermal) ionization levels are the values of the Fermi level at which energies of competing charge states cross.

In dealing with charged defects when using a periodic supercell approach, the long-range Coulomb interaction has to be treated carefully. The Coulomb interactions between the charged defects in the periodic array produce a divergent term in the total energy per unit cell of the system. In order to avoid this unphysical situation, the unit cell was implicitly neutralized by compensating the extra or missing (relative to the neutral state) electron charge on the defect with a rigid background charge, which is uniformly spread over the whole unit cell. (The background charge does not enter the expressions for the exchange and correlation energies.) In principle this could cause some systematic errors, but as long as the supercell is large enough, any spurious interdefect interactions or other effects of the background charge are expected to be small.³⁰

As a check of the charged-defect calculations, we performed 16-atom and 32-atom cell calculations for the antisite defect P_{Zn} . The thermal ionization energies of the antisite defect were extracted from the formation energy calculations as described above. The main results of the two supercell calculations are shown in Table I. The results exhibit similar trends in electronic structure. They predict that, when the Fermi level is near the valence-band edge, 3+ is the stable charge state of the antisite defect. They also agree in that both calculations predict that 1+, 2+, and 3+ charge states of the defect form a “negative-U” system. The reaction $2\text{P}_{\text{Zn}}^{2+} \rightarrow \text{P}_{\text{Zn}}^{1+} + \text{P}_{\text{Zn}}^{3+}$ is exothermic by 0.4 eV and by 0.3 eV in the 32-atom and

16-atom cell calculations, respectively, suggesting that the 2+ charge state is a metastable state, as discussed in Sec. III B below.

III. CALCULATIONAL RESULTS AND DISCUSSION

A. Summary of defect configurations

We now turn to the details of our calculations on defects in ZnSe. In this section, we summarize our results for the stable ionic configurations of defects (P and N) in their various charge states. For a given defect state, all ionic coordinates in the supercell were fully relaxed, using the calculated Hellmann-Feynman forces, to determine the stable ionic configuration for the defect state.

The distortion induced by the presence of a defect in ZnSe can be conceptually divided into two components: a breathing relaxation, which preserves the tetrahedral (T_d) symmetry of the host material, and a Jahn-Teller (JT) distortion, which reduces the symmetry. When the JT effect is present, the symmetry of the defect system is reduced to C_{3v} or C_{2v} , depending on the electronic structure of the system. Our calculations indicate that, with the exceptions of negatively charged states of interstitial defects P_{int} and N_{int} , the induced displacements of next-nearest neighbors are much smaller than those of the nearest-neighbor atoms of the impurities. Therefore, in this section we report only the displacements of the nearest neighbors.

When only breathing relaxations are induced, the defect system stabilizes into a configuration with T_d symmetry, which we describe in terms of the bond length z between the impurity and its nearest neighbors, the angle between any two such bonds being 109.5° . When a C_{3v} JT distortion is also present, we define z to be the length of the unique (axial) bond between the impurity and its neighbors, z' to be the length of the other three equivalent (basal) bonds, and θ to be the angle between the axial and basal bond. The notations are illustrated in Fig. 1(a).

For the case of a C_{2v} distortion, the impurity atom

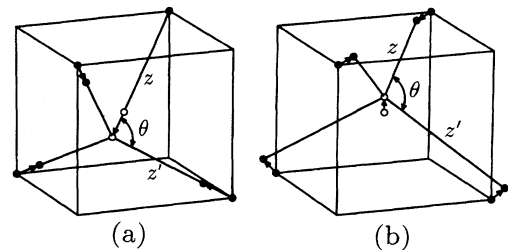


FIG. 1. (a) Definitions of quantities z , z' , and θ for C_{3v} defect configurations. (b) Same for C_{2v} defects. Open and filled circles represent impurity and neighboring host atoms, respectively.

TABLE I. The thermal ionization levels (relative to the VBM) of the antisite defect P_{Zn} , and reaction energy of $2\text{P}_{\text{Zn}}^{2+} \rightarrow \text{P}_{\text{Zn}}^{1+} + \text{P}_{\text{Zn}}^{3+}$ (positive is exothermic), calculated for supercells containing the defect in 32-atom and in 16-atom cell geometries.

	32-atom cell	16-atom cell
3+/1+	0.71 eV	0.45 eV
1+/0	1.71 eV	2.01 eV
$2\text{P}_{\text{Zn}}^{2+} \rightarrow \text{P}_{\text{Zn}}^{1+} + \text{P}_{\text{Zn}}^{3+}$	+0.41 eV	+0.27 eV

moves in the [001] direction, making two bond lengths shorter and two longer. For this case, we define z and z' to be the two different bond lengths, and θ to be the angle between the bonds with different bond lengths, as shown in Fig. 1(b). Ionic configurations with C_{2v} symmetry are found to be relatively rare. They occur for neutral states of P and N interstitials, for which threefold degenerate states (not counting spin) in the band gap are partially occupied by three electrons. However, the departures from the breathing-relaxed (T_d) structure are very small.

The results of our calculations for the stable configurations of defects (P and N) in their various charge states are summarized in Table II. The choice of charge states will be explained later in Secs. III B and III C, where the defects are discussed in more detail. As many of our results for P have been presented previously,¹⁸ the discussions of P defects in the next two sections shall be concentrated on reviewing and expanding upon the most important findings.

B. P_{Zn} and N_{Zn}

We first discuss the case when an impurity occupies a Zn site (antisite defect). The neutral antisite defect P_{Zn} has a fully occupied a_1 (nondegenerate) level and a singly occupied t_2 (threefold-degenerate) level in the band gap. Since we are mainly interested in the p -type material, we considered 0 (neutral) to 3+ charge states for the antisite

P. For positively charged states of the defect, substantial breathing relaxations (which preserve T_d symmetry) are found with the change of charge state as shown in Table II. Our calculation suggests that, because of these strong relaxations, the states P_{Zn}^{1+} , P_{Zn}^{2+} , and P_{Zn}^{3+} form a “negative-U system”³¹ as illustrated in Fig. 2. The reaction $2P_{Zn}^{2+} \rightarrow P_{Zn}^{1+} + P_{Zn}^{3+}$ is exothermic by 0.4 eV, so that the 2+ charge state is a metastable state.

With tetrahedral symmetry imposed, the neutral N_{Zn} has a threefold-degenerate (t_2) level in the band gap, occupied by a single electron. This is in contrast to the case of the neutral P_{Zn} , whose a_1 level is in the gap as well (see above). This difference in the electronic structure can be understood roughly by the trend in the sp^3 average energy of P and N are about -6 and -10 eV, respectively, relative to that of Zn. The lowest conduction band of bulk ZnSe originates from the antibonding combination of Zn 4s and 4p orbitals with surrounding Se orbitals. Since the sp^3 average energy of the impurity P atom is substantially lower than that of the Zn atom, the a_1 and t_2 defect states, which also have antibonding character with the surrounding Se orbitals, are lowered and appear in the band gap. In the case of N_{Zn} , whose sp^3 average energy is even lower than P, only the t_2 state appears in the gap, as the a_1 state has descended into the valence band.

The singly occupied t_2 level of N_{Zn} is near the midgap,

TABLE II. Stable configurations of defects in ZnSe in various charge states. The definitions of z , z' , and θ are given in the text and in Fig. 1, and are different for C_{3v} and C_{2v} configurations. Given in the parentheses is the “breathing-relaxed” bond length, i.e., that between the impurity and its nearest neighbors when T_d symmetry is imposed. For reference, the bond length of bulk ZnSe is 2.45 Å. E_{JT} represents the energy lowering from the Jahn-Teller distortion. Results for P_{Se} and N_{Se} from Ref. 17 are included for completeness.

Defect	Charge	Structure	z (Å)	z' (Å)	θ (°)	(Å)	E_{JT} (eV)
P_{Se}	1-	T_d	2.29		109.5	(2.29)	
	0	C_{3v}	2.40	2.30	107.7	(2.33)	0.04
	1+	C_{3v}	2.57	2.31	105.4	(2.35)	0.15
P_{Zn}	0	C_{3v}	2.33	2.66	113.7	(2.54)	0.16
	1+	T_d	2.50		109.5	(2.50)	
	2+	T_d	2.39		109.5	(2.39)	
	3+	T_d	2.24		109.5	(2.24)	
$P_{int}(T_{Zn})$	2-	C_{3v}	2.32	2.33	109.7	(2.33)	
	1-	C_{3v}	2.32	2.40	110.9	(2.39)	0.03
	0	C_{2v}	2.45	2.45	109.5	(2.45)	
	1+	C_{3v}	3.70	2.55	75.4	(2.54)	1.18
	2+	C_{3v}	3.34	2.64	84.7	(2.58)	0.63
N_{Se}	3+	C_{3v}	3.22	2.66	88.1	(2.65)	0.44
	1-	T_d	1.96		109.5	(1.96)	
	0	$\sim T_d$	1.95		109.5	(1.95)	
	1+	$\sim T_d$	1.94		109.5	(1.94)	
N_{Zn}	1-	C_{3v}	1.78	2.65	121.3	(2.31)	1.03
	0	C_{3v}	1.88	2.46	116.1	(2.27)	0.37
	1+	T_d	2.21		109.5	(2.21)	
$N_{int}(T_{Zn})$	3-	T_d	1.91		109.5	(1.91)	
	2-	C_{3v}	1.96	1.95	109.2	(1.95)	
	1-	C_{3v}	2.02	2.01	109.0	(2.02)	
	0	C_{2v}	2.06	2.06	109.5	(2.06)	

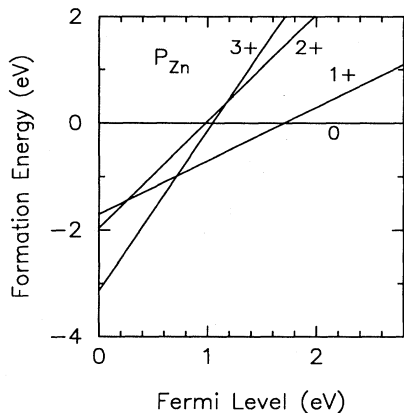


FIG. 2. Formation energies of antisite P_{Zn} defects in different charge states, relative to P_{Zn}^0 , as a function of the Fermi-level position.

and we thus consider 1- to 1+ charge states for p type ZnSe. The breathing-relaxed bond lengths between N and neighboring Se atoms of the 1- and neutral states of N_{Zn} were calculated to be 2.31 and 2.27 Å, respectively. For these states, additional strong JT distortions were found, resulting in C_{3v} -symmetry structures. The negatively charged defect lowers its energy by 1.03 eV by the JT distortion, in which the N impurity moves 0.53 Å toward a nearest-neighbor Se atom, expanding the bond lengths with the other three by 0.34 Å. For the neutral defect, it lowers its energy by 0.37 eV by moving 0.39 Å toward a nearest-neighbor Se atom. These distortions are favorable because the energy of the electrons in the gap states is lowered by the distortions. The JT distortion does not occur for the 1+ charged state, since the gap states are empty. The present calculation indicates that the thermal ionization energies for 1+/0 and 0/1- transitions are 1.0 and 1.1 eV, respectively, with respect to the VBM.

C. P_{int} and N_{int}

An impurity can assume two possible tetrahedral interstitial sites in ZnSe, one surrounded by Zn atoms (T_{Zn}), the other by Se atoms (T_{Se}). We consider only the former, since our calculations indicate that for P and N impurities it is energetically favorable. For instance, in the breathing-relaxed structure, N_{int}^0 at the T_{Zn} site is 1.4 eV lower in total energy than at the T_{Se} site.

The neutral P and N interstitials at the T_{Zn} site are found to have an almost threefold-degenerate level in the band gap, with a very small splitting due to a JT distortion. The level is partially occupied by three electrons. According to our LDA calculation the level of P is deep in the band gap, whereas that of N is near the VBM, suggesting that the N interstitial at the T_{Zn} site should form a shallow acceptor state.

Remarkably, for the P interstitial, we find that

the total-energy difference between the tetrahedral and hexagonal interstitial sites is strongly charge-state dependent. For negatively charged and neutral (2- to 0) states, we have found relatively small relaxations of the nearest-neighbor Zn atoms, indicating that the T_{Zn} site is stable for these charge states. For the positively charged states (1+ to 3+), on the other hand, the tetrahedral site is unstable with respect to sites near the hexagonal interstitial site. For instance, for the 1+ state, the P atom moves in the [111] direction by about 1.2 Å from its ideal position, almost reaching the hexagonal site, and this minimum-energy site is 1.2 eV more stable than the T_{Zn} site.

For the N defect at the T_{Zn} site, we consider 0 (neutral) to 3- charge states, since the gap level is shallow and partially occupied by three electrons. The ionic configurations of N interstitial defects can be characterized by strong breathing relaxations of the nearest-neighbor Zn atoms and very minor JT distortions, as shown in Table II. For the 3- state, the neighboring Zn atoms relaxed by 0.54 Å from their ideal positions toward the N impurity. JT distortion did not occur, as the gap level is completely filled. For 2- and 1- charge states we have found very weak JT distortions of C_{3v} symmetry, with very minor departures from T_d symmetry. The neutral defect, as expected from the fact that it has three electrons in the gap level, assumes a C_{2v} structure, but the associated distortion is again very small. We also find substantial outward relaxations of the six second-nearest-neighbor Se atoms, by 0.27, 0.23, 0.19, and 0.18 Å for 3-, 2-, 1-, and neutral states, respectively. The calculated thermal depths relative to the VBM for 0/1-, 1-/2-, and 2-/3- are 0.06, 0.17, and 0.30 eV, respectively.

D. Formation energies of the P and N defects

We now discuss our results for the formation energies of the P and N defects. In this paper, we use a convention in which μ_{Se}^{bulk} sets the zero of μ_{Se} . Thus, when μ_{Se} is only slightly negative, it corresponds to a Se-rich condition, while a value close to -2.79 eV corresponds to a Zn-rich condition. The appropriate value of μ_{Se} for stoichiometric ZnSe ought to fall somewhere in the middle of this range. Unfortunately, a determination of the precise value of μ_{Se} for stoichiometric ZnSe would require exhaustive calculations on native defects in ZnSe, which we have not undertaken. We have adopted the expedient of choosing $\mu_{Se} = -1.4$ eV (the middle of the allowed range) to represent "stoichiometric" ZnSe in the calculations reported in this paper.

From the formation energy calculations of the P defects¹⁸ we have found that, when the Fermi level is at 0.6 eV or higher above the valence-band edge, the Se substitutional site is most favored by P in stoichiometric ZnSe, as it has the lowest formation energy. However, as the Fermi level moves down and approaches the valence-band edge, the formation energy of the antisite defect P_{Zn} in the 3+ charge state is comparable to or lower than that of the substitutional P_{Se} in the neutral or 1- charge state. This result suggests that when shallow acceptors (P_{Se}^0) are created, they are compensated by P_{Zn} ,

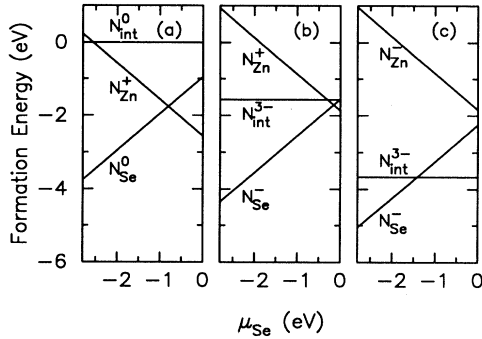


FIG. 3. Formation energies of nitrogen impurities, relative to $N_{\text{int}}^0(T_{\text{Zn}})$, as a function of the Se chemical potential for three characteristic Fermi levels: (a) 0.0 eV, (b) 0.7 eV, and (c) 1.4 eV above the VBM.

which act as donors.

In the case of the N impurity, contrary to the P case, the formation energy of the antisite defect N_{Zn} turns out to be higher than that of the substitutional N_{Se} for stoichiometric ZnSe, indicating a minimal compensation of the holes by the antisite defect. This can be in part attributed to the fact that N_{Zn} assumes the 1+ charge state even in the heavily doped p type ZnSe. While the formation energy of P_{Zn} in the 3+ charged state decreases quickly as the Fermi level moves down in the band gap, that of N_{Zn} in the 1+ charge state decreases much more slowly.

Our results for the total energies of formation of the N_{Se} , N_{Zn} , and $N_{\text{int}}(T_{\text{Zn}})$ defects, plotted versus μ_{Se} over the estimated accessible range, are shown in Fig. 3. Since different charge states are also considered, Fig. 3 shows the results for three characteristic Fermi levels in p -type material: 0.0, 0.7, and 1.4 eV relative to the VBM. When the Fermi level is near the midgap, the formation energy of the $N_{\text{int}}^{3-}(T_{\text{Zn}})$ is comparable to that of the N_{Se}^{1-} at $\mu_{\text{Se}} \approx -1.4$ eV, while that of N_{Zn}^{1-} is much higher. As the Fermi level moves down in the band gap, the interstitial site becomes less and less favorable. For the Fermi level near the VBM, the formation energy of N substitutional defects is lower than the energies of the N antisite and interstitial defects at $\mu_{\text{Se}} \approx -1.4$ eV.

E. Role of defects in the doping problem

P and N impurities in ZnSe have been theoretically studied and discussed by several authors in conjunction with the p -type doping problem. Chadi and Chang studied column-V impurities (P and As) in ZnSe and suggested that these impurities could possess at least two distinct atomic configurations which give rise to a shallow effective-mass state and to a deeply localized state.¹⁴ In the shallow state the impurity is situated on a substitutional Se site and is fourfold coordinated. The deep state, which is either in the neutral or positively charged state, results from a large lattice relaxation in which a

bond between the impurity and one of the four neighboring Zn atoms is broken. Chadi and Chang find the shallow state is energetically unstable against the deep state, and suggest that the low conductivity of holes in P- and As-doped ZnSe is the result of a shallow-deep transition of acceptor states.¹⁴ N impurities, however, are proposed to give rise to a shallow acceptor state in either the small or large lattice-relaxed states.¹⁴

Our previous calculations¹⁷ support the existence of a shallow acceptor state associated with the fourfold-coordinated substitutional P impurity in ZnSe. However, we were unable to find the stable deep center characterized by a large lattice relaxation.

In this paper we propose that the antisite defect P_{Zn} plays a critical role in the doping problem. Our formation-energy calculation for phosphorus-doped stoichiometric ZnSe suggests that, when the Fermi level is near the valence-band edge as a result of phosphorus doping, the formation energy of the antisite defect P_{Zn} in the 3+ charge state is comparable to or lower than that of the substitutional P_{Se} in the neutral or 1- charge state. Therefore, when shallow acceptors (P_{Se}^0) are created, they are compensated by the donors (P_{Zn}). Since, near the valence-band edge, the stable charge state of the antisite defect is 3+, three acceptors are compensated by a single antisite defect.

According to the calculations by Laks *et al.* on native defects, the concentration of native defects in stoichiometric ZnSe is quite low (of order 10^{10} cm^{-3} at $T = 600$ K in material doped p type with 10^{18} cm^{-3} dopants).¹⁶ Thus, the equilibrium state is most likely determined by the concentrations of the dopant-associated defects. In the equilibrium state for which the concentrations of P_{Zn}^{3+} and P_{Se}^{1-} are the same order of magnitude, the calculated Fermi level lies at 0.4–0.5 eV above the VBM.³² In the equilibrium state, P_{Zn}^{3+} and P_{Se}^{1-} are the dominant impurities, and small concentrations of P_{Se}^0 and positively charged $P_{\text{int}}(H)$ with other intrinsic defects such as Zn interstitials and Zn vacancies are expected.

When the Se chemical potential is near its minimum allowed value, the formation energy of P_{Se}^0 becomes lower than that of P_{Zn} , indicating that the compensation of shallow acceptors by P_{Zn} would be suppressed. However, in this nonstoichiometric Zn-rich condition, compensation by Zn interstitials acting as double donors is expected instead.^{6,16} Thus, the p -type doping would probably not improve.

On the other hand, the calculation for the nitrogen defects indicates that substitutional nitrogen (which forms a shallow acceptor) is lower in formation energy than nitrogen antisite or interstitial defects. Therefore, even when the Fermi level is positioned near the valence-band edge as a result of heavy nitrogen doping, the concentrations of the antisite and the interstitial defects are expected to be too small to cause a substantial compensation of the free holes. These results suggest that nitrogen should be a more robust acceptor than phosphorus, which is consistent with the successful p type doping of ZnSe based on the introduction of nitrogen dopants.²

Figure 4 compares the trends in the relative forma-

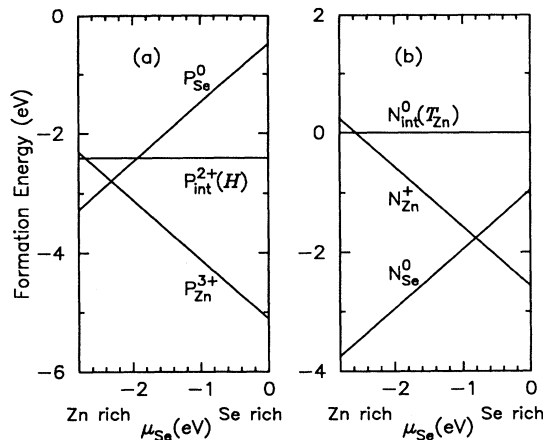


FIG. 4. Formation energies of (a) phosphorus and (b) nitrogen impurities as a function of the Se chemical potential, for the Fermi level at the VBM.

tion energies of phosphorus and nitrogen impurities in extreme p -type ZnSe (Fermi level at the VBM).

When impurities are injected in ZnSe, instead of occupying substitutional sites they may be combined with a constituent of ZnSe to form a certain chemical phase, thereby limiting the hole concentration. In their theoretical study on acceptor impurities (Li, Na, and N) in ZnSe,¹³ Van de Walle *et al.* investigated the solubility limits for the impurities, and found that the doping of ZnSe with Li and Na be limited by formation of the compounds Li_2Se and Na_2Se , respectively. However, for N, it turned out that the solubility did not pose a severe limitation for the hole concentration. They also investigated the competition between various N sites and found that N_{Zn} and N interstitials were much higher in formation energy than N_{Se} , in agreement with our calculational results.

For N doping, under optimal conditions, a net acceptor concentration of up to 10^{18} cm^{-3} has been achieved in ZnSe grown by molecular-beam epitaxy using an active nitrogen beam generated by a free radical source.² The actual nitrogen concentrations in these ZnSe samples, however, have been measured to be 3–10 times larger than the free-hole concentrations, suggesting that under high nitrogen incorporation rates significant amounts of compensating species exist in the material. Although the hole concentrations in the range of mid- 10^{17} cm^{-3} are acceptable for manufacturing the diode lasers, larger free-hole concentrations in p -type ZnSe are desirable, particularly to minimize the electrical contact problem.¹ Thus an issue of significant importance is to identify the defects causing the compensation and work towards reducing

their concentration. Regarding this problem, Chadi and Troullier propose that the low doping efficiency is caused by interstitial N in novel bonding configurations.¹¹ They have examined various interstitial bonding configurations of N such as a twofold bridge bonding, $\langle 110 \rangle$ -split and $\langle 100 \rangle$ -split interstitials, and find that the configurations give both shallow acceptor and shallow donor states. This might provide a mechanism to explain the observed self-compensation.

IV. SUMMARY

In summary, we have studied the electronic properties and relaxed ionic structures of phosphorus and nitrogen defects in ZnSe, using pseudopotential total-energy calculations within the local-density approximation to density-functional theory. Conventional norm-conserving pseudopotentials are not well suited to the study of ZnSe and other II-VI semiconductors, as the tightly bound cation d orbitals would require a very large plane-wave basis set. We employ instead an ultrasoft pseudopotential scheme, in which the problematic Zn $3d$ orbitals are included as valence states with a modest plane-wave cut-off energy of 25 Ry. This approach, combined with the conjugate-gradient technique for the minimization of the total-energy functional, enables us to study the defected ZnSe system efficiently and accurately. Various charge states of P and N defects are considered; their electronic states and ionic configurations are studied, and their formation energies are calculated.

The calculational results indicate that, for stoichiometric ZnSe material, the difficulty in doping ZnSe p type with phosphorus dopants is caused by compensation of the free holes by antisite defects P_{Zn} , which act as triple donors. In nonstoichiometric Zn-rich conditions, the compensation by P_{Zn} is expected to be suppressed, but the compensation of the holes by Zn interstitials is expected instead. Thus, the p -type doping would probably not improve. In the case of nitrogen doping, the concentrations of the antisite defect N_{Zn} and interstitial defect at the T_{Zn} site in stoichiometric ZnSe are expected to be too small to cause significant compensation of the free holes, which is consistent with the successful fabrication of p -type ZnSe material based on nitrogen doping.

ACKNOWLEDGMENTS

This work is supported by NSF Grant No. DMR-91-15342. Cray YMP time was provided by the National Center for Supercomputing Applications under Grant No. DMR920003N.

* Present address: School of Physics, Georgia Institute of Technology, Atlanta, GA 30332.

¹ G. F. Neumark, R. M. Park, and J. M. DePuydt, *Phys. Today* **47** (6), 26 (1994).

² J. Qiu, J. M. DePuydt, H. Cheng, and M. A. Haase, *Appl. Phys. Lett.* **59**, 2992 (1991), and references therein.

³ M. A. Haase, J. Qiu, J. M. DePuydt, and H. Cheng, *Appl. Phys. Lett.* **59**, 1272 (1991).

- ⁴ H. Jeon, J. Ding, A. V. Nurmikko, W. Xie, M. Kobayashi, and R. L. Gunshor, *Appl. Phys. Lett.* **60**, 892 (1992); H. Jeon, J. Ding, W. Xie, D. Grillo, W. Patterson, M. Kobayashi, R. L. Gunshor, and A. V. Nurmikko, *ibid.* **59**, 3619 (1992).
- ⁵ C. H. Henry, K. Nassau, and J. W. Shiever, *Phys. Rev. B* **4**, 2453 (1971).
- ⁶ R. W. Jansen and O. F. Sankey, *Phys. Rev. B* **39**, 3192 (1989).
- ⁷ G. F. Neumark, *J. Appl. Phys.* **51**, 3383 (1980).
- ⁸ S. Y. Ren, J. D. Dow, and S. Klemm, *J. Appl. Phys.* **66**, 2065 (1989).
- ⁹ J. D. Dow, R.-D. Hong, S. Klemm, S. Y. Ren, M.-H. Tsai, O. F. Sankey, and R. V. Kasowski, *Phys. Rev. B* **43**, 4396 (1991).
- ¹⁰ T. Sasaki, T. Oguchi, and H. Katayama-Yosida, *Phys. Rev. B* **43**, 9362 (1991).
- ¹¹ D. J. Chadi and N. Troullier, *Physica (Amsterdam)* **185B**, 128 (1993).
- ¹² G. F. Neumark, *Phys. Rev. Lett.* **62**, 1800 (1989).
- ¹³ C. G. Van de Walle, D. B. Laks, G. F. Neumark, and S. T. Pantelides, *Phys. Rev. B* **47**, 9425 (1993).
- ¹⁴ D. J. Chadi, *Appl. Phys. Lett.* **59**, 3589 (1991); D. J. Chadi and K. J. Chang, *ibid.* **55**, 575 (1989).
- ¹⁵ S. Y. Ren, J. D. Dow, and J. Shen, *Phys. Rev. B* **38**, 10 677 (1988).
- ¹⁶ D. B. Laks, C. G. Van de Walle, G. F. Neumark, P. E. Blöchl, and S. T. Pantelides, *Phys. Rev. B* **45**, 10 965 (1992).
- ¹⁷ K. W. Kwak, R. D. King-Smith, and D. Vanderbilt, *Phys. Rev. B* **48**, 17 827 (1993).
- ¹⁸ K. W. Kwak, D. Vanderbilt, and R. D. King-Smith, *Phys. Rev. B* **50**, 2711 (1994).
- ¹⁹ W. E. Pickett, *Comput. Phys. Rep.* **9**, 115 (1989).
- ²⁰ K. C. Haas and D. Vanderbilt, in *Proceedings of the 18th International Conference on the Physics of Semiconductors*, edited by O. Engstrom (World Scientific, Singapore, 1987), p. 1181.
- ²¹ G. E. Engel and R. J. Needs, *Phys. Rev. B* **41**, 7876 (1990).
- ²² J. L. Martin, N. Troullier, and S.-H. Wei, *Phys. Rev. B* **43**, 2213 (1991).
- ²³ D. Vanderbilt, *Phys. Rev. B* **41**, 7892 (1990).
- ²⁴ K. W. Kwak, R. D. King-Smith, and D. Vanderbilt, *Physica (Amsterdam)* **B185**, 154 (1993).
- ²⁵ J. P. Perdew and A. Zunger, *Phys. Rev. B* **23**, 5048 (1981).
- ²⁶ D. J. Chadi and M. L. Cohen, *Phys. Rev. B* **8**, 5747 (1973).
- ²⁷ M. C. Payne, M. P. Teter, D. C. Allan, T. A. Arias, and J. D. Joannopoulos, *Rev. Mod. Phys.* **64**, 1045 (1992).
- ²⁸ R. D. King-Smith and D. Vanderbilt, *Phys. Rev. B* **49**, 5828 (1994).
- ²⁹ G.-X. Qian, R. M. Martin, and D. J. Chadi, *Phys. Rev. B* **38**, 7649 (1988).
- ³⁰ C. G. Van de Walle, P. J. H. Denteneer, Y. Bar-Yam, and S. T. Pantelides, *Phys. Rev. B* **39**, 10 791 (1989).
- ³¹ P. W. Anderson, *Phys. Rev. Lett.* **34**, 953 (1975).
- ³² This was calculated for μ_{Se} in the middle of its accessible range, $\mu_{Se} \approx -1.4$ eV.